

UC Berkeley

UC Berkeley Previously Published Works

Title

Beyond Expectation: Advanced Materials Design, Synthesis, and Processing to Enable Novel Ferroelectric Properties and Applications

Permalink

<https://escholarship.org/uc/item/7d91919q>

Journal

MRS Advances, 5(64)

ISSN

2731-5894

Authors

Kim, Jieun
Lupi, Eduardo
Pesquera, David
[et al.](#)

Publication Date

2020-12-01

DOI

10.1557/adv.2020.344

Peer reviewed



Beyond Expectation: Advanced Materials Design, Synthesis, and Processing to Enable Novel Ferroelectric Properties and Applications

Jieun Kim¹, Eduardo Lupi¹, David Pesquera^{1,2}, Megha Acharya^{1,3}, Wenbo Zhao¹, Gabriel A. P. Velarde¹, Sinead Griffin⁴, Lane W. Martin^{1,4}

1. *Department of Materials Science & Engineering, University of California, Berkeley, Berkeley, CA 94720*
2. *Catalan Institute of Nanoscience and Nanotechnology, Campus UAB, Bellaterra, 08193 Barcelona, Spain*
3. *Materials Sciences Division, Lawrence Berkeley National Laboratory, Berkeley, CA 94720*
4. *Molecular Foundry, Lawrence Berkeley National Laboratory, Berkeley, CA 94720*

ABSTRACT

Ferroelectrics and related materials (e.g., non-traditional ferroelectrics such as relaxors) have long been used in a range of applications, but with the advent of new ways of modeling, synthesizing, and characterizing these materials, continued access to astonishing breakthroughs in our fundamental understanding come each year. While we still rely on these materials in a range of applications, we continue to re-write what is possible to be done with them. In turn, assumptions that have underpinned the use and design of certain materials are progressively being revisited. This perspective aims to provide an overview of the field of ferroelectric/relaxor/polar-oxide thin films in recent years, with an emphasis on emergent structure and function enabled by advanced synthesis, processing, and computational modeling.

INTRODUCTION:

Advances in the prediction/simulation, synthesis, characterization, and fabrication of ferroelectrics and related materials, in particular as thin films, have provided access to effects and possibilities once considered fantasy. This perspective will briefly review some recent highlights in the design, synthesis, and processing of ferroelectric and related materials, with an emphasis on thin films and on how these approaches are ushering the field in new and innovative directions. Within this context, the perspective is organized in six sections. In Section 1, we review some of the monumental breakthroughs in understanding of relaxors, approaches to improve their performance in conventional applications, and efforts to create novel functionalities. In Section 2, we cover recent efforts in “materials by design” that aim to identify new types of polar order, which can potentially coexist with exotic phenomena and function not found in classical ferroelectrics. In Section 3, we review theoretical predictions and experimental efforts focused on designing/synthesizing novel superlattice structures that permit emergent function and properties that are not expected from parent materials alone. In Section 4, we highlight new processing approaches to control properties through unconventional methods (*e.g.*, ion bombardment/irradiation, free-standing membranes). In Section 5, we review current research efforts on low-power, non-volatile memory and logic that are increasingly calling upon ferroelectrics. Finally, in Section 6, we end with an outlook which provides a snapshot of the ongoing research focus in the community and challenges that remain.

1. Complex-Polar Order – New Life for Relaxors

The ability to simulate and synthesize ferroelectric materials as thin films has enabled numerous watershed studies that have illuminated our understanding of these complex materials. Aided by further developments across this spectrum, similar approaches to the study of complex-ferroelectric relaxors are now being implemented. This section summarizes recent milestones and perspectives for advances in this regard.

1.1. New understanding of old materials

Although relaxors were discovered nearly six decades ago, their true polar structure is still a matter of discussion [1]. It is widely believed that nanometer-sized polar nanoregions (PNRs) are embedded in a paraelectric matrix and grow with decreasing temperature. This model was developed to help explain experimental observations of butterfly-shaped diffuse-scattering patterns, but recent molecular-dynamics simulations have presented an alternative vision of the nanoscale domain structure which can also reproduce key features of the diffuse scattering from the prototypical relaxor $(1-x)\text{PbMg}_{1/3}\text{Nb}_{2/3}\text{O}_3\text{-}(x)\text{PbTiO}_3$ (PMN-PT) [2]. In this work, it was proposed that relaxor behavior originates from the coexistence of ferroelectric- and paraelectric-like unit cells, whose dynamic character is determined by the unit-cell composition. This discovery led the authors to propose a new, “slush-like model” of polar structures (Fig. 1a), in which nanoscale domains are separated by low-angle domain walls, rather than by a paraelectric matrix.

Another recent breakthrough in understanding relaxors was made by systematic measurements of diffuse scattering in PMN-PT across the morphotropic phase boundary [3] which found previously unrecognized modulations in diffuse scattering caused by anion displacements. This was made possible by measuring diffuse scattering at high Q values using neutrons which revealed that the butterfly-shaped diffuse scattering

observed in X-ray measurements (Fig. 1b) becomes asymmetric at high Q (Fig. 1c), thus highlighting the critical role of oxygen displacements.

1.2. New experimental approaches

Among the various experimental techniques used to study the structure of relaxors, diffuse scattering is arguably the most important since it is highly sensitive to local inhomogeneities that abound in relaxors. One of the most common approaches to studying relaxors is to induce ferroelectric or paraelectric behavior by controlling experimental conditions. Recent advances in the ability to produce high-quality relaxors as thin films are now expanding the community's ability to exact this control [4]. In turn, synchrotron-based X-ray diffraction and new high-speed detectors now enable the collection of three-dimensional diffuse-scattering patterns which, in this case, were used to evaluate the strain-induced evolution of domain structure in PMN-PT films (Fig. 1d). Real-space visualization of dipole patterns suggest that the observed change in diffuse-scattering pattern from butterfly- to disc-shape is due to disordered domain walls where polarization rotates from up-poled domains to down-poled domains in a continuous manner.

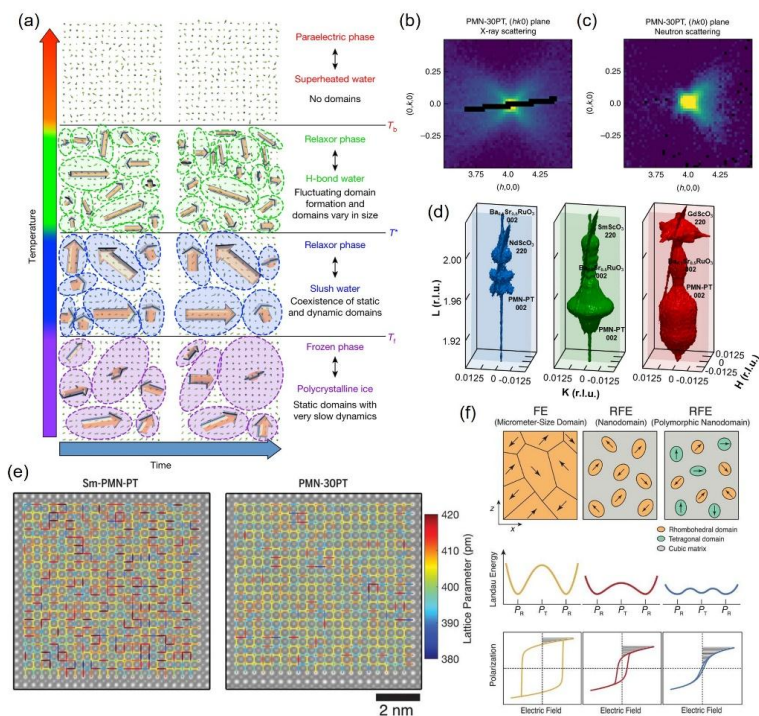


Figure 1. (a) Schematic of slush-like model for the phase transitions in relaxors (adapted from Ref. [2]). (b) Diffuse-scattering patterns in the 400 Brillouin zone are shown for (h, k, 0) measured at 100 K with X-rays and (c) measured at 6 K with neutrons (adapted from Ref. [3]). (d) 3D reciprocal space mapping about the PMN-PT 002-diffraction condition for heterostructures grown on NdScO₃, SmScO₃, and GdScO₃ (110)₀ substrates, corresponding to -0.5%, -1.0%, -1.5% compressive epitaxial strains, respectively (adapted from Ref. [4]). (e) Lattice parameter of A sublattice in Sm-PMN-PT and PMN-30PT crystals, respectively (adapted from Ref. [7]). (f) Comparative display of Landau energy profiles and P-E loops of a ferroelectric (FE) with micrometer-size domains, a relaxor ferroelectric (RFE) with nanodomains, and an RFE with polymorphic nanodomains. The shadowed area in the P-E loops represents the energy density (adapted from Ref. [13]).

The advent of epitaxial thin-film approaches is also opening new ways to perturb relaxor order. For example, finite size effects were previously studied in relaxor ceramics by controlling the average grain size [5]; however, it is challenging to control the grain structure down to sufficiently small sizes (on the order of a few nanometers) while maintaining high crystalline quality. Recent studies have now explored size effects in epitaxial thin films of the relaxor $\text{PbSc}_{0.5}\text{Ta}_{0.5}\text{O}_3$ [6] in order to understand what happens to PNRs when the average length scale of the material is on the same length scale of the domain size? In turn, it was found that the reduction of sample size and the resulting distribution of polar structures drives suppression and eventual quenching of the electrical response of relaxors, which may be attributed to increasing dipole-dipole and dipole-interface interactions.

At the same time, advances in atomic-resolution scanning transmission electron microscopy (STEM) techniques have proven to be extremely useful in providing understanding of the structural details, and by association, the underlying mechanisms of giant piezoelectricity in relaxors. Notably, high-angle annular dark field STEM (HAADF-STEM) images captured significant differences in the degree of structural disorder at the atomic scale in Sm-doped PMN-PT single crystals (Fig. 1e), which show nearly twice as high piezoelectric performance compared to undoped PMN-PT [7]. Moreover, recent developments of integrated differential phase contrast imaging demonstrated the potential to direct imaging of oxygen atom columns [8], which may play a significant role in giant piezoelectricity in relaxors [3].

1.3. New applications for relaxors

Relaxors continue to be best known for their superior electromechanical coupling, and, in fact, recent years have shown new routes to further improve their performance [7,9,10]. Besides these classic uses, new applications for relaxor thin films have emerged. For example, these materials were shown to be potentially important for waste-heat energy conversion via a process called pyroelectric energy conversion [11,12]. Using thin-film devices, researchers demonstrated large energy density, power density, and conversion efficiency of 1.06 J/cm^3 , 526 W/cm^3 and 19% of Carnot, respectively, which is equivalent to the performance of a thermoelectric device with an effective figure of merit $ZT = 1.16$ for a temperature change of 10 K [11]. The excellent performance in relaxor thin films was explained in terms of field-induced enhancement of the average polarization. This work pointed out several advantages of thin-film geometries, including the fact that significantly larger sweeps of electric field (achieved with much lower voltage in comparison to bulk materials) give rise to enhanced polarization changes. Furthermore, high-frequency and high-temperature-amplitude cycling is more readily achieved to increase power and work, respectively. In addition, significantly less heat input is required to increase the temperature of the lattice while still driving the same changes in the surface charge density with the applied voltage (*i.e.*, the advantage of thin films is that the effects at work scale with the area of the device, not the volume).

Another area of rapidly growing interest for relaxor thin films is the study of energy storage with dielectric capacitors. Although dielectric capacitors possess inherently fast charge-discharge rates, they have traditionally exhibited relatively low energy densities. In the last few years, researchers have worked to induce relaxor behavior while maintaining high polarization in materials as a way to break this trade-off [13]. The approach, called polymorphic nanodomain design (Fig. 1f), was used to realize the coexistence of rhombohedral and tetragonal nanodomains in a paraelectric matrix and large energy density (112 J/cm^3) with a high efficiency (80%). More recently, researchers have used defect engineering in relaxors to extend their breakdown strength – thus greatly

increasing their energy storage density (133 J/cm^3) while maintaining high efficiency ($>75\%$), reliability ($>10^8$ cycles), and temperature stability (-100 to 200°C) [14]. Such approaches could be used to design new relaxor materials from known ferroelectric and paraelectric materials or extend the function of already “good” materials, both of which are promising for finding ultrahigh performance relaxor materials.

2. Exotic-Polar Order and Function – From Dream to Reality

Advances in first-principles approaches have enabled a revolution in the design of functional materials – including ferroelectrics [15]. In order to identify novel ferroelectric materials, crystallographic group-theory relations are employed in determining energy-lowering polar distortions in non-polar prototype structures [16–18] while modelling Hamiltonians with “artisanal” *ab initio* calculations. Combined model Hamiltonian and first-principles calculations have been especially invaluable in unravelling complex order parameter spaces present in well-known ferroelectrics⁴ [19,20] such as BaTiO_3 , PbTiO_3 (Fig. 2a), and BiFeO_3 (Fig. 2b) which rely on acentric displacement of *A* or *B* site cations with respect to the BO_6 octahedra in the ABO_3 perovskite structure [21]. Ferroic order, however, has also been realized indirectly using non-polar ordering.

2.1. Materials by design

Improper ferroelectrics exhibit non-polar structural distortions (*e.g.*, zone-boundary octahedral tilting) or magnetic order which drive a breaking of spatial-inversion symmetry and result in a spontaneous polarization. To recognize such unique polarity, researchers have applied *ab initio* calculations using group theory [22] with invariant analysis [23] and energy-lowering structural distortions [24]. Further, trilinear coupling (*i.e.*, a combination of two non-polar lattice distortions in a parent centrosymmetric phase which can induce a polar degree of freedom) has been identified to play a role in YMnO_3 [25], LuFeO_3 [26] (Fig. 2c), Ruddlesden-Popper $\text{Ca}_3\text{Mn}_2\text{O}_7$ [27], Dion-Jacobson $\text{CsNdNb}_2\text{O}_7$ [28], and artificial superlattices such as $(\text{PbTiO}_3)_n/(\text{SrTiO}_3)_n$ [29]. In YMnO_3 , the ferroelectric behavior is due to the buckling of the layered MnO_5 polyhedra, causing displacement of the yttrium ions. Similarly, in LuFeO_3 , the structural shift in the Lu- O_2 layer with respect to the Fe-O layer is responsible for the long-range polar order. Coupling the long-range polar order with magnetic order (*e.g.*, in BiFeO_3 , YMnO_3 , $\text{Ca}_3\text{Mn}_2\text{O}_7$, LuFeO_3) leads to the emergence of magnetoelectric multiferroics (*i.e.*, the presence of spontaneous polarization and magnetization which can be reoriented by applying magnetic and electric fields, respectively). Besides probing fundamental mechanisms, controls such as strain, chemical alloying, and applied fields are now routinely explored in DFT for achieving new phases and properties which have been experimentally validated [29–31]. The key advantages are exploring large combinatorial regions of phase space more efficiently than experiment and identifying metastable states of interest to lead experimental approaches.

2.2. Expanding the repertoire of polar materials

An interesting case where theory and computation have driven materials discovery is in predicting new polar metals, which possess supposedly contradictory properties: polarity (electric-dipole ordering) and metallic behavior (mobile-charge carriers) [32–35]. Though conduction electrons are expected to screen the long-range electrostatic interactions in the lattice, they were found to not interact strongly with the

transverse optical phonons and the Lorentz-local fields which, in turn, results in ferroelectricity [36]. Some of the known examples include $\text{Cd}_2\text{Re}_2\text{O}_7$ [37] and LiOsO_3 [32]. In fact, the family of LiXO_3 ($X = \text{V}, \text{Nb}, \text{Ta}, \text{Os}$) materials have been proposed to form a new class of so-called hyperferroelectrics with an unstable phonon mode driving the ferroelectric distortion. Guided by theoretical studies, (111)-oriented films of the metal NdNiO_3 with a polar (Pc) structure have been synthesized by controlling the octahedral tilt patterns [38] (Fig. 2d-f). Such an approach can be extended to identify new multifunctional materials for interesting applications like anisotropic thermoelectric response, magnetoelectric multiferroics [39], topological phases, spin textures, non-centrosymmetric superconductivity, etc. – properties which are possible due to the cooperative interactions between ferroelectric order and several order parameters (e.g., charge, spin, orbitals).

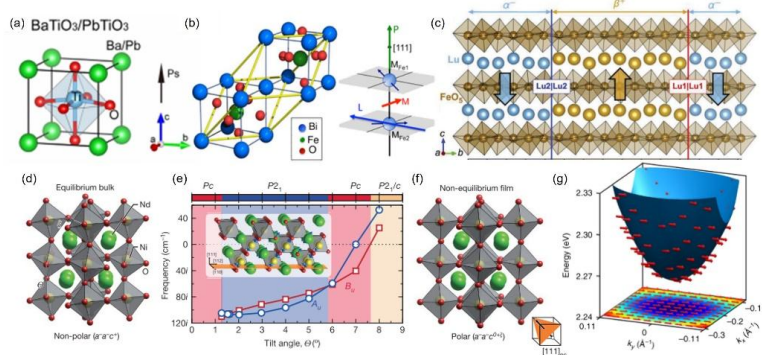


Figure 2. (a) Crystal structure of bulk BaTiO_3 ($P4mm$) and PbTiO_3 ($P4mm$). (b) Crystal structure of bulk BiFeO_3 ($R3c$) and schematic illustration of the direction of anti-ferromagnetic spins (MFe) within the (111) planes with respect to direction of spontaneous polarization (P) (adapted from Ref. [21]). (c) Crystal structure of bulk LuFeO_3 ($P63cm$) illustrating the structural distortion of Lu ion relative to FeO_5 polyhedra resulting in the breaking of spatial inversion symmetry (adapted from Ref. [26]) (d) Crystal structure of bulk non-polar NdNiO_3 (e) Calculated zone-center phonon mode for centrosymmetric NdNiO_3 on LaAlO_3 (111) substrate as a function of change in NiO_6 tilt angle. Imaginary frequencies indicate dynamical lattice instabilities, which harden as the tilt angle θ increases to obtain the non-equilibrium polar structure. (f) Crystal structure of polar NdNiO_3 as a thin-film on LaAlO_3 (111) substrate (adapted from Ref. [38]). (g) Schematic illustration of persistent spin texture near the conduction band minimum in BiInO_3 ($\text{Pna}21$) crystal structure (adapted from Ref. [41]).

2.2. Expanding the repertoire of polar materials

An interesting case where theory and computation have driven materials discovery is in predicting new polar metals, which possess supposedly contradictory properties: polarity (electric-dipole ordering) and metallic behavior (mobile-charge carriers) [32–35]. Though conduction electrons are expected to screen the long-range electrostatic interactions in the lattice, they were found to not interact strongly with the transverse optical phonons and the Lorentz-local fields which, in turn, results in ferroelectricity [36]. Some of the known examples include $\text{Cd}_2\text{Re}_2\text{O}_7$ [37] and LiOsO_3 [32]. In fact, the family of LiXO_3 ($X = \text{V}, \text{Nb}, \text{Ta}, \text{Os}$) materials have been

proposed to form a new class of so-called hyperferroelectrics with an unstable phonon mode driving the ferroelectric distortion. Guided by theoretical studies, (111)-oriented films of the metal NdNiO_3 with a polar (Pc) structure have been synthesized by controlling the octahedral tilt patterns [38] (Fig. 2d-f). Such an approach can be extended to identify new multifunctional materials for interesting applications like anisotropic thermoelectric response, magnetoelectric multiferroics [39], topological phases, spin textures, non-centrosymmetric superconductivity, etc. – properties which are possible due to the cooperative interactions between ferroelectric order and several order parameters (e.g., charge, spin, orbitals).

2.3. Quantum phenomena in topological ferroelectrics

Furthermore, polar structures with strong spin-orbit coupling (SOC) could host exotic quantum phenomena (e.g., Weyl semimetalllicity, Rashba-Dresselhaus spin splitting, metal-to-insulator transitions, etc.) [40]. Combining SOC with a crystal structure exhibiting nonsymmorphic space-group symmetry (e.g., BiInO_3 ; $Pna2_1$) has been predicted to give rise to persistent-spin texture near the conduction-band minimum [41] (Fig. 2g). Another tantalizing possibility is control and coupling of ferroic-order parameters with topological phenomena [42]. Several candidates with coexisting topological and ferroelectric properties have been proposed by theory (e.g., a strain-induced topological insulating phase in ferroelectric CsPbI_3 [43], a topological insulating phase in electron-doped BaBiO_3 [44], and nodal-line semimetals in hexagonal manganites [45]), however, to date none have been experimentally demonstrated. As has been pointed out, this is a cautionary tale in materials prediction; many of these dream material properties arise in material chemistries which are simply not stable or feasible for synthesis [46]. New advances, however, in *ab initio* synthesizability indicators, feedback and integration with experiment, and fully automated synthesis workflows, will address many of these current drawbacks in *ab initio* prediction [47].

3. Novel Emergent Function – One Plus One, Does Not Necessarily Equal Two

Pushing the limits of materials functionality means adding more degrees of freedom in materials synthesis. Here, we examine the role of superlattice heterostructuring as an approach that has garnered renewed interest in recent years due to its ability to elicit novel and emergent function in ferroelectric systems. The key is the ability of such approaches to drive competition between relevant energy terms that can be manipulated by counterpoising dissimilar materials (be that in lattice parameter, order parameter magnitude, dielectric constant, etc.) at the unit-cell level.

3.1 Dielectric/ferroelectric heterostructures: emergent-polar order

While many ferroelectric-based heterostructures and superlattices have been studied to date, by far the most extensively studied system are $(\text{PbTiO}_3)_n/(\text{SrTiO}_3)_n$ (where n is the number of unit cells) superlattices wherein the resulting structure varies as a function of the superlattice periodicity. Emergent order such as improper ferroelectricity was reported in short-period superlattices ($n < 10$) [29], flux-closure domains in long-period superlattices ($n > 20$) [48], and polar vortices and skyrmions in intermediate-period superlattices ($10 < n < 20$) [49–51], [52]. These vortices and skyrmions have attracted considerable attention due to their continuously evolving polar order. At the atomic scale, polar skyrmions (as illustrated by atomic-scale mapping of the polarization, Fig. 3a-c) are

characterized by diverging (top surface) and converging (bottom surface) Néel skyrmions (hedgehog-like) with a Bloch-wall structure at the waist. Taken together, this complex 3D structure was determined to have a skyrmion number of +1. 4D-STEM imaging has confirmed the hedgehog-like structure (Fig. 3d,e), with signal and polarization maps matching simulations (Fig. 3f,g). The complex polarization structures arise from the interaction of the strongly polar PbTiO_3 layer with the insulating and dielectric, but non-polar, SrTiO_3 layers that sandwich it as well as the elastic boundary conditions imposed by the substrate. This complex competition between polarization, elastic, electrostatic, and gradient energies drives the material into a state unlike anything seen in ferroelectrics before. These polarization topologies pose a great opportunity to study the behavior of multi-dimensional polarization structures and the potential for how applied electric fields can manipulate and control the skyrmion structure. Initial studies are also showing that these heterostructures can exhibit novel phase transitions and enhanced susceptibilities. For example, superlattices with polar vortices and skyrmions exhibit signatures of non-classical phase transitions (that deviate strongly from Curie-Weiss-type behavior) as well as dielectric permittivity that greatly exceeds what is expected for series-capacitor or more complex equivalent-circuit models for such structures (thus leading to reports of negative capacitance) [53]. Increasing interest on the concept of negative capacitance has also been driven by studies on multidomain ferroelectrics [54] and work on metal/ $\text{Hf}_{0.5}\text{Zr}_{0.5}\text{O}_2/\text{Ta}_2\text{O}_5$ /metal heterostructures wherein transient negative capacitance in a monodomain ferroelectric with a resistor in series has been shown [55]. The design of this structure exposes the downward concavity in the center of the double-well structure of a standard ferroelectric system (Fig. 3h), which can be reconstructed from polarization hysteresis loops. Such reports pave the way for further investigation into the potential for using superlattice heterostructure to manipulate the energy landscape of ferroelectric materials thereby producing new phenomena.

3.2. Ferroelectric/ferroelectric heterostructures: engineering unexpected properties

Even placing a ferroelectric next to another ferroelectric can bring about novel effects. Research efforts have leveraged polarization rotation [56], inversion symmetry breaking [57], and phase-field simulations [58] as a pathway to design and optimize piezoelectric responses. For example, a recent study [59] placed two different ferroelectric phases in the $\text{PbZr}_{1-x}\text{Ti}_x\text{O}_3$ system (from the rhombohedral zirconium-rich and from the tetragonal titanium-rich sides of the phase diagram) and used superlattice design as a proxy for local composition – asking what happens when the overall chemistry is that of the morphotropic phase boundary (MPB), but the individual layers are far away from that boundary? The intimate interfacing of these dissimilar materials resulted in a unique combination of effects: simultaneous large polarization magnitude and large permittivity. The material effectively acted like a combination of the robust parent ferroelectrics and an interfacial region that looked like the MPB phase. The common theme of novel synthesis techniques is unit-cell precise deposition, in this case by RHEED-assisted pulsed-laser deposition (Fig. 3i), provides a pathway to design novel heterostructures and thus access interfacial-driven phenomena.

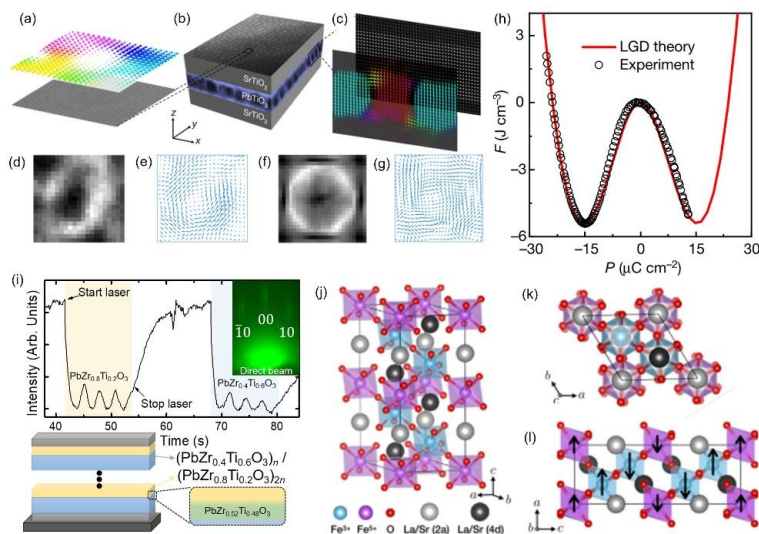


Figure 3. (a,b,c) Displacement maps of Ti atoms extracted from HAADF-STEM images of a $(\text{PbTiO}_3)_n/(\text{SrTiO}_3)_n$ superlattice. (d,e) 4D-STEM image showing a polar skyrmion-bubble, as recreated by (f,g) multislice simulations (adapted from Ref. [52]). (h) Free energy of $\text{Hf}_{0.5}\text{Zr}_{0.5}\text{O}_2\text{-Ta}_2\text{O}_5$ highlighting the downward concavity between the double well shape (adapted from Ref. [55]). (i) Growth of ferroelectric superlattice $(\text{PbZr}_{0.4}\text{Ti}_{0.6}\text{O}_3)_n/(\text{PbZr}_{0.8}\text{Ti}_{0.2}\text{O}_3)_n$ with in situ RHEED-monitoring (adapted from Ref. [59]). (j) Arrangement of atoms in the $\text{La}_{1/3}\text{Sr}_{2/3}\text{FeO}_3$ system showing charge order in multi-valent Fe ions. (k) Oxygen octahedral rotations and (l) antiferromagnetic order from different viewpoints (adapted from Ref. [60]).

3.3. Superlattice-induced-ferroelectricity: beyond conventional ferroelectrics

Approaches to induce emergent ferroelectric order have been previously explored in the context of octahedral rotations in perovskite materials, which has led to the aforementioned improper ferroelectricity in short-period $(\text{PbTiO}_3)_n/(\text{SrTiO}_3)_n$ superlattices. Recent DFT predictions have also reported that it might be possible to induce ferroelectricity by leveraging charge-order in mixed-valence solid solutions like $\text{La}_{1/3}\text{Sr}_{2/3}\text{FeO}_3$ [60]. This is accomplished by heterostructure design that combines *A*-site superlattice layering with a mixed valence (and continuous) *B*-site. These electrostatic interfacial distortions lead to the breaking of centrosymmetry and a corresponding ferroelectric ground state. This proof of concept paves the way for future research in the realization of novel approaches to ferroelectricity stemming from interfacial interactions, which will continue to be more relevant as devices get smaller. Such predictions also push experimentalists to ever more exacting control, posing the question of whether we can really achieve control at a single unit-cell level and lock in the chemical ordering and structure that is desired. Such questions will motivate the community's further pursuit of these matters.

4. Processing for Unprecedented Control – Ferroelectrics Like You’ve Never Seen Them

Advances in the synthesis of ferroelectric oxides are enabling researchers to obtain materials with ever improving crystalline quality and low concentrations of grown-in defects while offering advanced users fine-level control over structure, stoichiometry, and interfaces. But even under optimally controlled conditions, the resultant properties of these high-quality materials and the platforms on which they are fabricated are often not ideal for the desired applications. New post-synthesis processing approaches offer strategies to “fix one’s mistakes” by optimizing properties and integrating their functionalities into heterogenous devices combining materials that are incompatible via direct synthesis. In parallel, the progress in the design of ferroelectric-based nanodevices has enabled the development of new electromechanical and electrothermal platforms that aim at improving energy-conversion capabilities. Here we highlight a few of these novel processing approaches for the deterministic control of properties and the design of multifunctional devices.

4.1. Defect engineering via ion bombardment

The use of ion bombardment to generate point defects is a common processing technique applied in semiconductors to controllably create intergap states [61,62]. While defects in oxides can be purposely introduced *in situ* during synthesis by tuning from optimal growth conditions, post-synthesis bombardment and implantation methods provide for precise control over the amount and type of defects induced, as well as their spatial distribution.

In recent years, point-defect engineering via ion bombardment has been used to tailor properties and structures in ferroelectric films. Uniform irradiation of high-energy helium ions has been used to correct deficiencies in the “pristine” material, including high leakage currents, by trapping free carriers that contribute to conduction [63]. On the other hand, low-energy helium implantation was shown to introduce *strain doping* that can be exploited to modulate the competition between different crystal phases (Fig. 4a) and is expected to significantly enhance piezoelectric response [64]. Lastly, focused-ion beams were used to locally induce defects with nanometer precision, which allowed for the introduction of domain-nucleation centers [65] and for the creation of regions of increased domain-wall pinning [66], thus providing for local control of the switching process and the stabilization of multiple polarization states that could be used to design high-density multilevel memory devices (Fig. 4b). In general, ion-beam methods have been incorporated into the extensive toolbox of methods to fine-tune properties of ferroelectric oxides and are expected to continue to provide a useful approach for improving device performance [14].

4.2. Device integration via epitaxial lift-off

Another processing technique inherited from the semiconductor community is epitaxial lift-off [67]. This process involves the epitaxial growth of a film onto a sacrificial layer that can be selectively dissolved to produce a free-standing layer. Only recently have adequate sacrificial layers with high etching selectivity and crystalline quality been developed for perovskite oxides [68,69]. This, in combination with polymer-support transfer processes that preserve the film integrity after its release from the substrate, is now opening new doors for materials control (Fig. 4c). For example, it can enable highly sought after heterointegration of single-crystal oxide films on

semiconducting substrates by circumventing the complications of direct epitaxial growth caused by the lattice, thermal, and chemical mismatch between materials. Using this approach, successful integration of transistors with ferroelectric gates on silicon [68] as well as ferroelectric tunnel junctions on both silicon [70] and flexible polymers [71] were demonstrated.

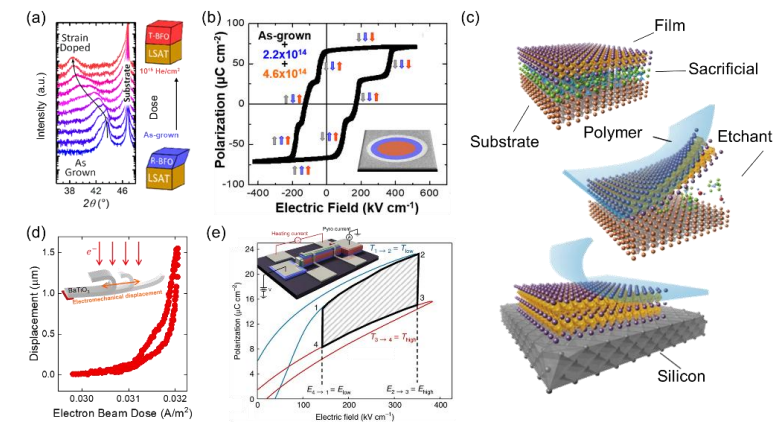


Figure 4. (a) Low-energy (4 keV) helium implantation can tune the competition between morphotropic phases in BiFeO₃ (adapted from Ref. [64]). (b) Higher energy (25 keV) focused helium bombardment can stabilize multiple switching steps in PbZr_{0.7}Ti_{0.3}O₃ capacitors (adapted from Ref. [66]). (c) Schematic of the epitaxial lift-off transfer process (adapted from Ref. [76]). (d) A giant electromechanical coupling is demonstrated in freestanding single-crystal BaTiO₃ membranes by observing the membranes folding induced by an electron beam with variable flux (adapted from Ref. [81]). (e) Direct, phase-sensitive electrothermal test platform devices (inset) provide a means for exploring energy conversion efficiencies, e.g. by performing pyroelectric Ericsson cycles (adapted from Ref. [11]).

Alternative processes for heterointegration have also been demonstrated via remote epitaxy through graphene layers [72] which allows for the release of epitaxial films using mechanical exfoliation and via epitaxial growth on muscovite substrates (termed as “van der Waals epitaxy” [73]) which enables the fabrication of flexible-ferroelectric devices [74]. All these synthesis processes avoid strong bonding of the films with the substrate, thus expanding the combinatorial approaches to fabricate multifunctional devices. Beyond this, the film-transfer methods also provide opportunities to explore new phases/properties when approaching the two-dimensional limit [75,76], target enhancement of properties typically clamped by the substrate in epitaxial systems [72], and provide mechanical control of properties and domain structures beyond the current limitations of heteroepitaxy [77,78]. These processing techniques are a “hot” field of work and new exciting studies are expected to appear in the next few years.

4.3. New opportunities for energy-conversion devices

The advances in processing of ferroelectric thin films are expected to directly impact the development of new, more efficient energy harvesters. In particular, devices with large electromechanical coupling are of high interest to power devices within the guise of the internet-of-things by converting mechanical vibrations into electrical energy. Among these, microelectromechanical systems (MEMS) consisting of piezoelectric/silicon bimorph cantilevers have shown the largest coupling coefficients under low-voltage operation [79]. Alternatively, the use of the ubiquitous flexoelectric effect in non-piezoelectric materials to actuate MEMS provides a means to avoid non-linear and temperature-dependent effects albeit with lower response [80]. Pioneering studies on the piezoresponse of freestanding-ferroelectric membranes fabricated via epitaxial lift-off have recently shown giant domain-driven electromechanical effects (Fig. 4d) [81], which, upon proper device processing, could pave the way for ultra-efficient MEMS. The exceptional mechanical flexibility demonstrated in these membranes [82] is concomitant to continuous dipole rotations coupled to large strain gradients, which could lay the groundwork for enhanced flexoelectric effects in ferroelectric (and dielectric) oxides.

There has also been renewed interest in the development of pyroelectric materials to harvest waste heat, with the main focus on the design and fabrication of AC phase-sensitive thin-film electrothermal test platforms capable of direct measurements of electrothermal effects (Fig. 4e, inset) [83]. Such approaches are shedding new light on this relatively understudied realm of physics in ferroelectric oxides. Free from convoluting effects of spurious, thermally stimulated currents which have long plagued previous characterization approaches for thin films, the “true” pyroelectricity can now be measured accurately in capacitor structures that are compatible with thin films and are providing robust insights into previously neglected effects such as dielectric and extrinsic domain-wall contributions to pyroelectricity [84,85]. Furthermore, with today’s thin-film processing strategies like the aforementioned defect engineering, greater electric fields and temperatures may be applied at increasing frequencies – going well beyond what can be physically obtained in bulk materials [66] and thus improving the pyroelectric performance. Additionally, with the ongoing developments in thin-film MEMS and lift-off techniques, devices may be fabricated on free-standing beams allowing for the direct investigation of secondary effects (*i.e.*, arising from thermally driven shape changes which couple via the piezoelectricity to drive changes in polarization with temperature) to pyroelectricity which have not been directly studied. On top of that, with relaxed mechanical restraints, these freestanding structures stand poised to enable the investigation of adapted thermodynamic Ericsson cycles for next-generation waste-heat converters. Namely, in addition to cycling applied electric field and temperature (Fig. 4e), small probe stresses via atomic force microscopy tips may be applied in-phase with temperature oscillations to provide insights into novel energy conversion mechanisms via multiple coupled functionalities, as well as produce enhanced energy and power densities not achievable in pure pyroelectric or (flexo-)piezoelectric energy generators.

5. Next-Generation Devices and Applications – Ferroelectrics Strike Back

With the rapid development of computing applications, researchers are motivated to develop novel low-energy devices for information processing. The impetus for this is grounded in the requirements of Dennard scaling for MOSFETs which roughly states that as transistors get smaller, for their power density to stay constant requires that the voltage be reduced by 30% with every generation [86]. Due to issues like current leakage at small sizes, however, Dennard scaling was abandoned around 2005-2007, even though the transistor sizes and counts in integrated circuits are still shrinking and growing, respectively, following Moore's law [87]. The breakdown of Dennard scaling has caused urgent demand for novel high-performance computational materials that can enable low-voltage operation.

5.1. Low-voltage and multi-state memory

Among candidate systems in this regard, ferroelectrics have shown great potential for low-voltage, non-volatile, and (even) multi-state memory and logic devices. There is a growing call for research to study ferroelectrics at the length, time, and energy scales required to provide for a paradigm shift in information technologies – namely understanding effects at the length scale of 1-10 nm, time scales less than 1 ns, and energy scales approaching 1-100 aJ per operation. This is an area ripe for impact and the application of new modeling, synthesis, fabrication, and characterization methods. Recent years have shown intriguing effects, for instance, in ultra-thin materials. For example, crystal orientation control in films of the canonical ferroelectric $\text{PbZr}_{0.2}\text{Ti}_{0.8}\text{O}_3$ showed that the scaling exponent in the evolution of coercive field with thickness (typically given by the Janovec-Kay-Dunn law, wherein $E_c \propto d^{-2.3}$ where d is the film thickness) can be decreased, on account of slight modifications of the crystal structure that enable lower-energy (non-180°) switching pathways [88]. On the other hand, by engineering domain structures, stable multi-state polarization values can be achieved, which provide a pathway for beyond binary function and potential neuromorphic operation [89–91].

5.2. New logic concepts: majority gate logic, MESO, and related

Building on the advances of the last decades in this regard, industry has taken a renewed interest in such ferroic materials to develop new concepts for next-generation memory and logic function. For example, the magnetoelectric spin-orbit (MESO) device (Fig. 5a,b) has been introduced as a potential choice for replacing or enhancing traditional complementary metal-oxide-semiconductor (CMOS) transistors [92]. This device has set challenging metrics for the field: a switching energy of 1-10 aJ per operation, switching voltages of <100 mV, and enhanced logic densities (by a factor of 5) compared with CMOS transistors. Further benefiting from nonvolatility, MESO is useful for both logic and memory devices, also known as a logic-in-memory device, enabling simplified computing structures and energy savings by avoiding the transfer of information from the logic to the memory and back. In turn, ever more elaborate logic architectures are being proposed based on these ideas, including majority-gate concepts [93].

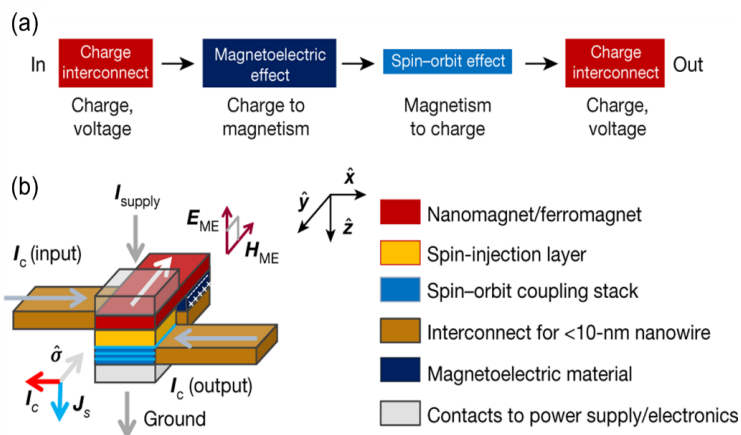


Figure 5. (a) Transduction of state variables for a cascaded charge-input and charge-output logic device. The magnetoelectric effect transduces the input information to magnetism, and the spin-orbit effect in a topological material transduces the magnetic state variable back to charge. (b) MESO device formed with a magnetoelectric capacitor and a topological material (adapted from Ref. [92]).

5.3. The rise of $h\bar{f}o_2$ and related materials

In parallel, considerable research and development effort has focused on understanding and utilizing the ferroelectric order reported in binary oxides such as doped HfO_2 , which are compatible with existing CMOS processes [94,95]. Hafnia-based ferroelectrics (and other similar binary systems) exhibit robust polarization stability (albeit with large coercive fields) and the potential for multi-state function [96]. The observations in this regard have opened the door to a range of new ferroelectric materials – including new 2D systems, nitrides, and more. What is clear, is that researchers will continue to call upon ferroelectrics for a range of applications in the years to come and these materials are strong candidates to play an important role in next-generation logic and memory applications.

6. What Does the Future Hold?

The future of thin-film ferroelectric materials is bright. From continued work on the discovery of novel materials to ways to push the limits of material function to the realization of a new generation of devices based on these materials, the near-term future will explore the limits of functionality, integration, and beyond.

6.1. *New materials, faster and faster*

Despite arriving at the 100-year anniversary of ferroelectrics, most research and nearly all applications are focused on just a handful of materials. This begs the question of what else is out there? The community is increasingly embracing resources like the *Materials Project* and others and leveraging innovative high-throughput discovery and design approaches to push new candidate materials. While it might be possible to identify thousands and thousands of new candidate materials, it remains unlikely that experimentalists can (or even should) make all of them. Combined efforts to streamline this process and identify new and better ways to computationally evaluate synthesizability are key. Armed with this, one can expect continued contributions in the form of new polymer, small-molecule ferroelectric crystals, hybrid perovskites, 2D transition-metal dichalcogenides (and other 2D materials) with the potential for ferroelectric order. Looking another 100 years in the future, hopefully there will be new materials we didn't even know about today.

6.2. *Beyond Moore's Law – a place at the table*

As noted above, ferroelectrics are likely to find a place in next-generation application in memory and logic operation. The question remains, however, what materials and in what form. Continued work on creating ideal versions of these materials will help push down switching energies and voltages, attention to synthesis will enable deterministic control of structure and interfaces and computational approaches will provide insights on how to tune switching phenomena and open the doors to achieve the desired functions in these materials. In just the last few years, a marked increase in the interest and demonstration of ferroelectrics in many forms in realistic devices suggests this is going to be a reality.

6.3. *Dissimilar materials integration*

One of the hanging questions for the future of ferroelectrics is whether they can be made compatible with the devices of tomorrow. Continued work on the integration of oxide ferroelectrics on semiconductors is thus important, but new advances like the lift-off process and pick-and-place approaches stand poised to enable the integration of ferroelectrics and a range of dissimilar materials. Whether it is placing ferroelectrics on-demand in CMOS stacks or creating new interfaces and heterostructures with other 2D materials (such as chalcogenides) or even mixing non-classical nitride-based ferroelectrics with the above, there is a nearly limitless potential for impact and development in this regard. That work could, in turn, lay the foundation for greatly expanding the types of materials used in commercial electronics and open new possibilities for device designers.

6.4. *The limits for ferroelectric function*

Still another open question for these ideas is how we can extend our already deep understanding of ferroelectrics to the length, time, and energy scales that are important for real applications. In this regard, the community needs to address the question of how we can produce, process, and study materials at length (both thickness and lateral), time, and energy scales that approach 1-10 nm, < 1 ns, and 1-100 aJ, respectively? This calls for advances and concerted efforts in modeling, synthesis, fabrication, and characterization using a diverse range of techniques. Be it operation in a

logic device or in 5G (and beyond) communications technologies, there is often a gap between traditional academic research and understanding of the needs of advanced technology. Finding ways to address this gap – melding understanding and questions from both directions – in the research of any class of materials is key for impact.

6.5. *New horizons*

Finally, as it always has been, there are likely to be new horizons for what ferroelectrics can contribute to. The growth and attention to, for example, quantum computing and beyond von Neumann computation should motivate the field to explore what roles this diverse set of materials could play. From core to auxiliary function of novel systems, the functionality that this versatile class of materials exhibits has great potential for impact.

ACKNOWLEDGEMENTS

The authors acknowledge the support of the Army Research Office under grant W911NF-14-1-0104, the U.S. Department of Energy, Office of Science, Office of Basic Energy Sciences, under Award Number DE-SC-0012375 and Materials Sciences and Engineering Division under Contract No. DE-AC02-05-CH11231 (Materials Project program KC23MP) for the development of ferroelectric materials, the National Science Foundation under grants DMR-1608938 and DMR-1708615, and the Intel Corp. via the FEINMAN program. D.P. acknowledges funding from the European Union's Horizon 2020 research and innovation programme under the Marie Skłodowska-Curie grant agreement No. 797123.

References:

- [1] J. Hlinka, *J. Adv. Dielect.* **02**, 1241006 (2012).
- [2] H. Takenaka, I. Grinberg, S. Liu, and A. M. Rappe, *Nature* **546**, 391 (2017).
- [3] M. J. Krogstad, P. M. Gehring, S. Rosenkranz, R. Osborn, F. Ye, Y. Liu, J. P. C. Ruff, W. Chen, J. M. Wozniak, H. Luo, O. Chmaissem, Z.-G. Ye, and D. Phelan, *Nat. Mater.* **17**, 718 (2018).
- [4] J. Kim, H. Takenaka, Y. Qi, A. R. Damodaran, A. Fernandez, R. Gao, M. R. McCarter, S. Saremi, L. Chung, A. M. Rappe, and L. W. Martin, *Adv. Mater.* **31**, 1901060 (2019).
- [5] J. Carreaud, P. Gemeiner, J. M. Kiat, B. Dkhil, C. Bogicevic, T. Rojac, and B. Malic, *Phys. Rev. B* **72**, 174115 (2005).
- [6] A. Fernandez, J. Kim, D. Meyers, S. Saremi, and L. W. Martin, *Phys. Rev. B* **101**, 094102 (2020).
- [7] F. Li, M. J. Cabral, B. Xu, Z. Cheng, E. C. Dickey, J. M. LeBeau, J. Wang, J. Luo, S. Taylor, W. Hackenberger, L. Bellaiche, Z. Xu, L.-Q. Chen, T. R. ShROUT, and S. Zhang, *Science* **364**, 264 (2019).
- [8] A. Kumar, R. Dhall, and J. M. LeBeau, *Microsc. Microanal.* **25**, 1838 (2019).
- [9] F. Li, D. Lin, Z. Chen, Z. Cheng, J. Wang, C. Li, Z. Xu, Q. Huang, X. Liao, L.-Q. Chen, T. R. ShROUT, and S. Zhang, *Nat. Mater.* **17**, 349 (2018).
- [10] C. Qiu, B. Wang, N. Zhang, S. Zhang, J. Liu, D. Walker, Y. Wang, H. Tian, T. R. ShROUT, Z. Xu, L.-Q. Chen, and F. Li, *Nature* **577**, 350 (2020).
- [11] S. Pandya, J. Wilbur, J. Kim, R. Gao, A. Dasgupta, C. Dames, and L. W. Martin, *Nat. Mater.* **17**, 432 (2018).

- [12] S. Pandya, G. Velarde, L. Zhang, J. D. Wilbur, A. Smith, B. Hanrahan, C. Dames, and L. W. Martin, *NPG Asia Mater.* **11**, 26 (2019).
- [13] H. Pan, F. Li, Y. Liu, Q. Zhang, M. Wang, S. Lan, Y. Zheng, J. Ma, L. Gu, Y. Shen, P. Yu, S. Zhang, L.-Q. Chen, Y.-H. Lin, and C.-W. Nan, *Science* **365**, 578 (2019).
- [14] J. Kim, S. Saremi, M. Acharya, G. Velarde, E. Parsonnet, P. Donahue, A. Qualls, D. Garcia, and L. Martin, *Science* **369**, 81 (2020).
- [15] K. Alberi, M. B. Nardelli, A. Zakutayev, L. Mitas, S. Curtarolo, A. Jain, M. Fornari, N. Marzari, I. Takeuchi, M. L. Green, M. Kanatzidis, M. F. Toney, S. Butenko, B. Meredig, S. Lany, U. Kattner, A. Davydov, E. S. Toberer, V. Stevanovic, A. Walsh, N.-G. Park, A. Aspuru-Guzik, D. P. Tabor, J. Nelson, J. Murphy, A. Setlur, J. Gregoire, H. Li, R. Xiao, A. Ludwig, L. W. Martin, A. M. Rappe, S.-H. Wei, and J. Perkins, *J. Phys. D: Appl. Phys.* **52**, 013001 (2019).
- [16] K. F. Garrity, *Phys. Rev. B* **97**, 024115 (2018).
- [17] C. Capillas, E. S. Tasci, G. de la Flor, D. Orobengoa, J. M. Perez-Mato, and M. I. Aroyo, *Zeitschrift Für Kristallographie* **226**, 186 (2011).
- [18] J. W. Bennett and K. M. Rabe, *J. Sol. St. Chem.* **195**, 21 (2012).
- [19] Ph. Ghosez, X. Gonze, and J.-P. Michenaud, *GFER* **186**, 73 (1996).
- [20] R. E. Cohen, *Nature* **358**, 136 (1992).
- [21] J. T. Heron, D. G. Schlom, and R. Ramesh, *Appl. Phys. Rev.* **1**, 021303 (2014).
- [22] H. L. B. Boström, M. S. Senn, and A. L. Goodwin, *Nat. Commun.* **9**, 2380 (2018).
- [23] D. M. Hatch and H. T. Stokes, *J. Appl. Crystallogr.* **36**, 951 (2003).
- [24] A. Stroppa, P. Barone, P. Jain, J. M. Perez-Mato, and S. Picozzi, *Adv. Mater.* **25**, 2284 (2013).
- [25] B. B. Van Aken, T. T. M. Palstra, A. Filippetti, and N. A. Spaldin, *Nat. Mater.* **3**, 164 (2004).
- [26] P. Barrozo, D. R. Småbråten, Y. Tang, B. Prasad, S. Saremi, R. Ozgur, V. Thakare, R. A. Steinhardt, M. E. Holtz, V. A. Stoica, L. W. Martin, D. G. Schlom, S. M. Selbach, and R. Ramesh, *Adv. Mater.* 2000508 (2020).
- [27] A. T. Mulder, N. A. Benedek, J. M. Rondinelli, and C. J. Fennie, *Adv. Funct. Mater.* n/a (2013).
- [28] N. A. Benedek, *Inorg. Chem.* **53**, 3769 (2014).
- [29] E. Bousquet, M. Dawber, N. Stucki, C. Lichtensteiger, P. Hermet, S. Gariglio, J.-M. Triscone, and P. Ghosez, *Nature* **452**, 732 (2008).
- [30] S. Tinte, K. M. Rabe, and D. Vanderbilt, *Phys. Rev. B* **68**, 144105 (2003).
- [31] J. Wang, B. Wylie-van Eerd, T. Sluka, C. Sandu, M. Cantoni, X.-K. Wei, A. Kvasov, L. J. McGilly, P. Gemeiner, B. Dkhil, A. Tagantsev, J. Trodahl, and N. Setter, *Nat. Mater.* **14**, 985 (2015).
- [32] Y. Shi, Y. Guo, X. Wang, A. J. Princep, D. Khalyavin, P. Manuel, Y. Michiue, A. Sato, K. Tsuda, S. Yu, M. Arai, Y. Shirako, M. Akaogi, N. Wang, K. Yamaura, and A. T. Boothroyd, *Nat. Mater.* **12**, 1024 (2013).
- [33] N. A. Benedek and T. Birol, *J. Mater. Chem. C* **4**, 4000 (2016).
- [34] Y. Cao, Z. Wang, S. Y. Park, Y. Yuan, X. Liu, S. M. Nikitin, H. Akamatsu, M. Kareev, S. Middey, D. Meyers, P. Thompson, P. J. Ryan, P. Shafer, A. N'Diaye, E. Arenholz, V. Gopalan, Y. Zhu, K. M. Rabe, and J. Chakhalian, *Nat. Commun.* **9**, 1547 (2018).
- [35] A. Filippetti, V. Fiorentini, F. Ricci, P. Delugas, and J. Íñiguez, *Nat. Commun.* **7**, 11211 (2016).
- [36] D. Puggioni and J. M. Rondinelli, *Nat. Commun.* **5**, 3432 (2014).
- [37] I. A. Sergienko, V. Keppens, M. McGuire, R. Jin, J. He, S. H. Curnoe, B. C. Sales, P. Blaha, D. J. Singh, K. Schwarz, and D. Mandrus, *Phys. Rev. Lett.* **92**, 065501 (2004).
- [38] T. H. Kim, D. Puggioni, Y. Yuan, L. Xie, H. Zhou, N. Campbell, P. J. Ryan, Y. Choi, J.-W. Kim, J. R. Patzner, S. Ryu, J. P. Podkaminer, J. Irwin, Y. Ma, C. J. Fennie, M. S. Rzechowski, X. Q. Pan, V. Gopalan, J. M. Rondinelli, and C. B. Eom, *Nature* **533**, 68 (2016).
- [39] V. M. Edelstein, *Phys. Rev. Lett.* **75**, 2004 (1995).

- [40] C. Shekhar, A. K. Nayak, Y. Sun, M. Schmidt, M. Nicklas, I. Leermakers, U. Zeitler, Y. Skourski, J. Wosnitzer, Z. Liu, Y. Chen, W. Schnelle, H. Borrmann, Y. Grin, C. Felser, and B. Yan, *Nat. Phys.* **11**, 645 (2015).
- [41] L. L. Tao and E. Y. Tsybal, *Nat. Commun.* **9**, 2763 (2018).
- [42] J. He, D. Di Sante, R. Li, X.-Q. Chen, J. M. Rondinelli, and C. Franchini, *Nat. Commun.* **9**, 492 (2018).
- [43] S. Liu, Y. Kim, L. Z. Tan, and A. M. Rappe, *Nano Lett.* **16**, 1663 (2016).
- [44] B. Yan, M. Jansen, and C. Felser, *Nat. Phys.* **9**, 709 (2013).
- [45] S. F. Weber, S. M. Griffin, and J. B. Neaton, *Phys. Rev. Materials* **3**, 064206 (2019).
- [46] A. Zunger, *Nature* **566**, 447 (2019).
- [47] W. Sun, S. T. Dacek, S. P. Ong, G. Hautier, A. Jain, W. D. Richards, A. C. Gamst, K. A. Persson, and G. Ceder, *Sci. Adv.* **2**, e1600225 (2016).
- [48] Y. L. Tang, Y. L. Zhu, X. L. Ma, A. Y. Borisevich, A. N. Morozovska, E. A. Eliseev, W. Y. Wang, Y. J. Wang, Y. B. Xu, Z. D. Zhang, and S. J. Pennycook, *Science* **348**, 547 (2015).
- [49] A. K. Yadav, C. T. Nelson, S. L. Hsu, Z. Hong, J. D. Clarkson, C. M. Schlepütz, A. R. Damodaran, P. Shafer, E. Arenholz, L. R. Dedon, D. Chen, A. Vishwanath, A. M. Minor, L. Q. Chen, J. F. Scott, L. W. Martin, and R. Ramesh, *Nature* **530**, 198 (2016).
- [50] A. R. Damodaran, J. D. Clarkson, Z. Hong, H. Liu, A. K. Yadav, C. T. Nelson, S.-L. Hsu, M. R. McCarter, K.-D. Park, V. Kravtsov, A. Farhan, Y. Dong, Z. Cai, H. Zhou, P. Aguado-Puente, P. García-Fernández, J. Íñiguez, J. Junquera, A. Scholl, M. B. Raschke, L.-Q. Chen, D. D. Fong, R. Ramesh, and L. W. Martin, *Nat. Mater.* **16**, 1003 (2017).
- [51] Z. Hong, A. R. Damodaran, F. Xue, S.-L. Hsu, J. Britson, A. K. Yadav, C. T. Nelson, J.-J. Wang, J. F. Scott, L. W. Martin, R. Ramesh, and L.-Q. Chen, *Nano Lett.* **17**, 2246 (2017).
- [52] S. Das, Y. L. Tang, Z. Hong, M. a. P. Gonçalves, M. R. McCarter, C. Klewe, K. X. Nguyen, F. Gómez-Ortiz, P. Shafer, E. Arenholz, V. A. Stoica, S.-L. Hsu, B. Wang, C. Ophus, J. F. Liu, C. T. Nelson, S. Saremi, B. Prasad, A. B. Mei, D. G. Schlom, J. Íñiguez, P. García-Fernández, D. A. Muller, L. Q. Chen, J. Junquera, L. W. Martin, and R. Ramesh, *Nature* **568**, 368 (2019).
- [53] A. K. Yadav, K. X. Nguyen, Z. Hong, P. García-Fernández, P. Aguado-Puente, C. T. Nelson, S. Das, B. Prasad, D. Kwon, S. Cheema, A. I. Khan, C. Hu, J. Íñiguez, J. Junquera, L.-Q. Chen, D. A. Muller, R. Ramesh, and S. Salahuddin, *Nature* **565**, 468 (2019).
- [54] P. Zubko, J. C. Wojdeł, M. Hadjimichael, S. Fernandez-Pena, A. Sené, I. Luk'yanchuk, J.-M. Triscone, and J. Íñiguez, *Nature* **534**, 524 (2016).
- [55] M. Hoffmann, F. P. G. Fengler, M. Herzig, T. Mittmann, B. Max, U. Schroeder, R. Negrea, P. Lucian, S. Slesazek, and T. Mikolajick, *Nature* **565**, 464 (2019).
- [56] G. Liu, Q. Zhang, H.-H. Huang, P. Munroe, V. Nagarajan, H. Simons, Z. Hong, and L.-Q. Chen, *Adv. Mater. Interfaces* **3**, 1600444 (2016).
- [57] N. Sai, B. Meyer, and D. Vanderbilt, *Phys. Rev. Lett.* **84**, 5636 (2000).
- [58] F. Xue, J. J. Wang, G. Sheng, E. Huang, Y. Cao, H. H. Huang, P. Munroe, R. Mahjoub, Y. L. Li, V. Nagarajan, and L. Q. Chen, *Acta Mater.* **61**, 2909 (2013).
- [59] E. Lupi, A. Ghosh, S. Saremi, S. Hsu, S. Pandya, G. Velarde, A. Fernandez, R. Ramesh, and L. W. Martin, *Adv. Electron. Mater.* **6**, 1901395 (2020).
- [60] S. Y. Park, K. M. Rabe, and J. B. Neaton, *Proc. Natl. Acad. Sci. USA* **116**, 23972 (2019).
- [61] G. Dearnaley, *Nature* **256**, 701 (1975).
- [62] T. Shinada, S. Okamoto, T. Kobayashi, and I. Ohdomari, *Nature* **437**, 1128 (2005).
- [63] S. Saremi, R. Xu, L. R. Dedon, J. A. Mundy, S. L. Hsu, Z. Chen, A. R. Damodaran, S. P. Chapman, J. T. Evans, and L. W. Martin, *Adv. Mater.* **28**, 10750 (2016).

- [64] A. Herklotz, S. F. Rus, N. Balke, C. Rouleau, E. J. Guo, A. Huon, S. Kc, R. Roth, X. Yang, C. Vaswani, J. Wang, P. P. Orth, M. S. Scheurer, and T. Z. Ward, *Nano Lett.* **19**, 1033 (2019).
- [65] L. J. McGilly, C. S. Sandu, L. Feigl, D. Damjanovic, and N. Setter, *Adv. Funct. Mater.* **27**, (2017).
- [66] S. Saremi, R. Xu, F. I. Allen, J. Maher, J. C. Agar, R. Gao, P. Hosemann, and L. W. Martin, *Phys. Rev. Mater.* **2**, 084414 (2018).
- [67] M. Konagai, M. Sugimoto, and K. Takahashi, *J. Crystal Growth* **45**, 277 (1978).
- [68] S. R. Bakaul, C. R. Serrao, M. Lee, C. W. Yeung, A. Sarker, S.-L. Hsu, A. K. Yadav, L. Dedon, L. You, A. I. Khan, J. D. Clarkson, C. Hu, R. Ramesh, and S. Salahuddin, *Nat. Commun.* **7**, 10547 (2016).
- [69] D. Lu, D. J. Baek, S. S. Hong, L. F. Kourkoutis, Y. Hikita, and H. Y. Hwang, *Nat. Mater.* **15**, 1255 (2016).
- [70] D. Lu, S. Crossley, R. Xu, Y. Hikita, and H. Y. Hwang, *Nano Lett.* **19**, 3999 (2019).
- [71] Z.-D. Luo, J. J. P. Peters, A. M. Sanchez, and M. Alexe, *ACS Appl. Mater. Interfaces* **11**, 23313 (2019).
- [72] H. S. Kum, H. Lee, S. Kim, S. Lindemann, W. Kong, K. Qiao, P. Chen, J. Irwin, J. H. Lee, S. Xie, S. Subramanian, J. Shim, S. Bae, C. Choi, L. Ranno, S. Seo, S. Lee, J. Bauer, H. Li, K. Lee, J. A. Robinson, C. A. Ross, D. G. Schlom, M. S. Rzechowski, C.-B. Eom, and J. Kim, *Nature* **578**, 75 (2020).
- [73] Y.-H. Chu, *Npj Quantum Mater.* **2**, 67 (2017).
- [74] D. L. Ko, M. F. Tsai, J. W. Chen, P. W. Shao, Y. Z. Tan, J. J. Wang, S. Z. Ho, Y. H. Lai, Y. L. Chueh, Y. C. Chen, D. P. Tsai, L.-Q. Chen, and Y. H. Chu, *Sci. Adv.* **6**, eaaz3180 (2020).
- [75] S. S. Hong, J. H. Yu, D. Lu, A. F. Marshall, Y. Hikita, Y. Cui, and H. Y. Hwang, *Sci. Adv.* **3**, eaao5173 (2017).
- [76] D. Ji, S. Cai, T. R. Paudel, H. Sun, C. Zhang, L. Han, Y. Wei, Y. Zang, M. Gu, Y. Zhang, W. Gao, H. Huan, W. Guo, D. Wu, Z. Gu, E. Y. Tsymbal, P. Wang, Y. Nie, and X. Pan, *Nature* **570**, 87 (2019).
- [77] R. Xu, J. Huang, E. S. Barnard, S. S. Hong, P. Singh, E. K. Wong, T. Jansen, V. Harbola, J. Xiao, B. Y. Wang, S. Crossley, D. Lu, S. Liu, and H. Y. Hwang, *Nat. Commun.* **11**, 3141 (2020).
- [78] D. Pesquera, E. Parsonnet, A. Qualls, R. Xu, A. Gubser, J. Kim, Y. Jiang, G. Velarde, Y.-L. Huang, H. Hwang, R. Ramesh, and L. Martin, Submitted for Publication (2020).
- [79] S. H. Baek, J. Park, D. M. Kim, V. a. Aksyuk, R. R. Das, S. D. Bu, D. a. Felker, J. Lettieri, V. Vaithyanathan, S. S. N. Bharadwaja, N. Bassiri-Gharb, Y. B. Chen, H. P. Sun, C. M. Folkman, H. W. Jang, D. J. Kreft, S. K. Streiffer, R. Ramesh, X. Q. Pan, S. Trolrier-McKinstry, D. G. Schlom, M. S. Rzechowski, R. H. Blick, and C. B. Eom, *Science* **334**, 958 (2011).
- [80] U. K. Bhaskar, N. Banerjee, A. Abdollahi, E. Solanas, G. Rijnders, and G. Catalan, *Nanoscale* **8**, 1293 (2016).
- [81] H. Elangovan, M. Barzilay, S. Seremi, N. Cohen, Y. Jiang, L. W. Martin, and Y. Ivry, *ACS Nano* **14**, 5053 (2020).
- [82] G. Dong, S. Li, M. Yao, Z. Zhou, Y. Zhang, X. Han, Z. Luo, J. Yao, B. Peng, Z. Hu, H. Huang, T. Jia, J. Li, W. Ren, Z. Ye, X. Ding, J. Sun, C. Nan, L. Chen, J. Li, and M. Liu, *Science* **366**, 475 (2019).
- [83] S. Pandya, J. D. Wilbur, B. Bhatia, A. R. Damodaran, C. Monachon, A. Dasgupta, W. P. King, C. Dames, and L. W. Martin, *Phys. Rev. Appl.* **7**, 034025 (2017).
- [84] S. Pandya, G. A. Velarde, R. Gao, A. S. Everhardt, J. D. Wilbur, R. Xu, J. T. Maher, J. C. Agar, C. Dames, and L. W. Martin, *Adv. Mater.* **31**, 1803312 (2019).
- [85] G. Velarde, S. Pandya, L. Zhang, D. Garcia, E. Lupi, R. Gao, J. D. Wilbur, C. Dames, and L. W. Martin, *ACS Appl. Mater. Interfaces* **11**, 35146 (2019).
- [86] R. H. Dennard, F. H. Gaensslen, H.-N. Yu, V. L. Rideout, E. Bassous, and A. R. LeBlanc, *IEEE J. Solid-State Circuits* **9**, 256 (1974).
- [87] M. Bohr, *IEEE Solid-State Circuits Newsl.* **12**, 11 (2007).

- [88] R. Xu, R. Gao, S. E. Reyes-Lillo, S. Saremi, Y. Dong, H. Lu, Z. Chen, X. Lu, Y. Qi, S.-L. Hsu, A. R. Damodaran, H. Zhou, J. B. Neaton, and L. W. Martin, *ACS Nano* **12**, 4736 (2018).
- [89] W. Huang, W. Zhao, Z. Luo, Y. Yin, Y. Lin, C. Hou, B. Tian, C.-G. Duan, and X.-G. Li, *Adv. Electron. Mater.* **4**, 1700560 (2018).
- [90] W. Zhao, W. Huang, C. Liu, C. Hou, Z. Chen, Y. Yin, and X. Li, *ACS Appl. Mater. Interfaces* **10**, 21390 (2018).
- [91] R. Xu, S. Liu, S. Saremi, R. Gao, J. J. Wang, Z. Hong, H. Lu, A. Ghosh, S. Pandya, E. Bonturim, Z. H. Chen, L. Q. Chen, A. M. Rappe, and L. W. Martin, *Nat Commun* **10**, 1282 (2019).
- [92] S. Manipatruni, D. E. Nikonov, C.-C. Lin, T. A. Gosavi, H. Liu, B. Prasad, Y.-L. Huang, E. Bonturim, R. Ramesh, and I. A. Young, *Nature* **565**, 35 (2019).
- [93] Z. Liang, M. G. Mankalale, J. Hu, Z. Zhao, J.-P. Wang, and S. S. Sapatnekar, *IEEE J. Explor. Solid-State Comput. Devices Circuits* **4**, 51 (2018).
- [94] P. Buragohain, A. Erickson, P. Kariuki, T. Mittmann, C. Richter, P. D. Lomenzo, H. Lu, T. Schenk, T. Mikolajick, U. Schroeder, and A. Gruverman, *ACS Appl. Mater. Interfaces* **11**, 35115 (2019).
- [95] S. S. Cheema, D. Kwon, N. Shanker, R. dos Reis, S.-L. Hsu, J. Xiao, H. Zhang, R. Wagner, A. Datar, M. R. McCarter, C. R. Serrao, A. K. Yadav, G. Karbasian, C.-H. Hsu, A. J. Tan, L.-C. Wang, V. Thakare, X. Zhang, A. Mehta, E. Karapetrova, R. V. Chopdekar, P. Shafer, E. Arenholz, C. Hu, R. Proksch, R. Ramesh, J. Ciston, and S. Salahuddin, *Nature* **580**, 478 (2020).
- [96] K. Lee, H.-J. Lee, T. Y. Lee, H. H. Lim, M. S. Song, H. K. Yoo, D. I. Suh, J. G. Lee, Z. Zhu, A. Yoon, M. R. MacDonald, X. Lei, K. Park, J. Park, J. H. Lee, and S. C. Chae, *ACS Appl. Mater. Interfaces* **11**, 38929 (2019).